The published manuscript is available at Future Medicinal Chemistry via:
https://www.future-science.com/doi/10.4155/fmc-2022-0235

Investigation of halogenated furanones as inhibitors of quorum sensing-regulated bioluminescence in *Vibrio harveyi*

Jorge Pinheiro[1,2]*, Thérèse Lyons[3]*, Vanessa Las Heras[1,2], Miguel Villoria Recio[1,2], Cormac G. M. Gahan[1,2,3], and Timothy P. O'Sullivan[3,4,5].

*These authors contributed equally.

Affiliation

[1]School of Microbiology, University College Cork, Cork, Ireland, [2]APC Microbiome Ireland, University College Cork, Cork, Ireland; [3]School of Pharmacy, University College Cork, Cork, Ireland; [4]School of Chemistry, University College Cork, Cork, Ireland; [5]Analytical and Biological Chemistry Research Facility, University College Cork, Cork, Ireland.

Keywords: *Vibrio harveyi*, quorum sensing, bioluminescence, furanones, Suzuki, Sonogashira.

ABSTRACT

Aim: *Vibrio harveyi* is a Gram-negative marine bacterium which is a model system in the study of quorum sensing (QS). *V. harveyi* uses multichannel QS, mediated by three different signalling molecules. The aim of this study is to synthesise and screen a diverse series of furanones for their potential to inhibit *V. harveyi* quorum sensing. **Materials & methods:** A library of halogenated furanones was prepared and derivatised using standard Pd-mediated coupling reactions and subsequently evaluated for their effects on *V. harveyi* bioluminescence. **Results and Conclusion:** Several furanones inhibited QS-regulated bioluminescence, with *gem*-dichlorofuranone and tribromofuranone compounds proving especially effective. Importantly, a number of compounds were effective inhibitors of *V. harveyi* bioluminescence but did not have an impact on bacterial growth.

Introduction

V. harveyi is a Gram-negative marine bacterium which is pathogenic towards many marine animals [1]. The pathogen primarily affects shrimp but also negatively impacts fish, squid and lobsters [2-4]. It is the causative agent of luminescent vibrosis which results in significant losses in the aquaculture industry every year [5]. Part of the difficulty in dealing with *V. harveyi* lies in its ability to form biofilms which confer increased resistance to antimicrobials and biocides [6]. Biofilm-embedded bacteria are generally much more resistant than their planktonic equivalents [7]. Biofilm formation, as well as toxin production, are regulated in *V. harveyi* by a mechanism known as quorum sensing or QS [8, 9]. QS is an example of intracellular communication induced by signal molecules. These signal molecules, also known as autoinducers, are both produced and sensed by bacteria and regulate a variety of physiological processes, such as bioluminescence, biofilm formation and the production of virulence factors [10, 11].

V. harveyi is considered a model bacterium in the study of quorum sensing. It uses multichannel QS, mediated by three signalling molecules: an acyl homoserine lactone called *harveyi* autoinducer-1 (HAI-1), a furanosyl borate diester termed autoinducer-2 (AI-2) and a long-chain aminoketone known as cholera autoinducer-1 (CAI-1) [12, 13]. The three autoinducers are recognised by three sensor kinases in the cytoplasmic membrane. HAI-1 is recognised by LuxN, AI-2 is recognised by LuxQ (together with its binding protein LuxP) and CAI-1 is recognised by CqsS [14]. When little or no AI is present, the receptors undergo autophosphorylation and transfer phosphate to the transcriptional activator LuxO through the histidine phosphotransfer protein LuxU. This results in the transcription of regulatory sRNAs which, together with the RNA-binding protein Hfq, destabilise the mRNA of the master regulator LuxR. As a result, the LuxR protein is not produced and there is no bioluminescence. By contrast, when there is a high concentration of autoinducer present, the receptors switch from kinases to phosphatases. This allows for the dephosphorylation of LuxU and LuxO. Unphosphorylated LuxO is inactive and cannot promote the expression of sRNA's. This results in the stabilisation of luxR, leading to LuxR production and subsequent LuxR-mediated induction of genes which initiate bioluminescence and biofilm formation. Previous work by Anetzberger and co-workers revealed that, although *V. harveyi* produces all three autoinducers, their individual impact on QS-mediated bioluminescence is highly dependent on the growth phase of the bacteria [15]. Bioluminescence in the early and mid-exponential growth phase is attributed primarily to AI-2 as it is essentially the only autoinducer present. In the late exponential growth phase, bioluminescence is regulated by both AI-2 and HAI-1, while CAI-1 is typically not at its maximum level until the stationary phase. Overall, CAI-1 is thought to play a minor role in QS gene regulation [16].

Given the range of processes regulated by QS, and its intrinsic link with bacterial resistance, molecules which disrupt bacterial communication are the focus of much research [17]. Many of these molecules are based on bioactive natural products, such as those isolated from the marine algae *Delisea pulchra*, a red seaweed commonly found in Southern Australia [18]. This sub-tidal plant remains free of surface bacterial colonisation, due to its ability to produce a family of halogenated furanones, including fimbrolide **1** (Figure 1) [19]. The concentrations of these molecules in *Delisea pulchra* are inversely proportional to the quantity of bacteria that colonise the plant surface, suggesting that the compounds play a role in the inhibition of bacterial colonisation [20]. The endogenous furanones bear similarities to acylated homoserine lactones (AHL) such as **2** and can, unsurprisingly, result in disruption of AHL-controlled processes [21, 22]. Their biological effects may also be ascribed to their ability to inhibit the production of certain QS signals [23]. This is achieved by covalently binding to and inactivating the LuxS enzyme which is required for the biosynthesis of AI-2 [24]. Bacterial LuxS enzymes display a high degree of structural overlap and contain highly conserved active sites [25]. Additionally, Defoirdt and colleagues have suggested that structurally related thiophenones can inactivate the LuxR enzyme by a similar pathway [26].

Several groups, taking **1** as their lead, have synthesised and evaluated a wide range of structurally diverse furanones, dihyropyrrolones and thiophenones as QS inhibitors against various Gram-negative bacteria [27-30]. While simple mono- and dibromoolefins **3** and **4** have demonstrated potent biological effects in several species, their toxicity limits their potential as true QS inhibitors. In this paper, we outline the preparation of a library of furanone derivatives, incorporating a variety of aryl, alkylnyl and halogen substituents. Additionally, the development of a bromofuranone-cysteine conjugate is described. The effects of these compounds on *V. harveyi* quorum sensing-regulated bioluminescence are investigated, with several promising candidates subsequently identified which do not affect bacterial growth.

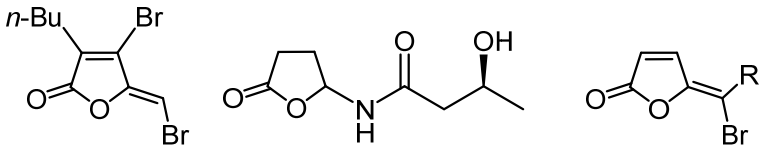

1 **2** **3** : R=H
4 : R=Br

Figure 1. Structures of fimbrolide (1), AHL (2) and bromofuranones 3 and 4.

Experimental Protocols

Chemistry

Compounds **6**-**22**, **27**-**28**, **30**, **33**-**37** and **39** were prepared using previously established procedures [31].

Synthesis of methylated furanones 23 and 24

To an oven-dried round bottom flask was added a mixture of **21/22** (211 mg, 0.787 mmol, 1 eq.), phenyl boronic acid (287 mg, 2.361 mmol, 3 eq.), tripotassium phosphate (501 mg, 2.361 mmol, 3 eq.), palladium(II) acetate (3 mg, 1 mol%), SPhos (2-dicyclohexylphosphino-2',6'-dimethoxybiphenyl) (7 mg, 2 mol%) and toluene (5 mL). The reaction mixture was heated to 100 °C for 4 hours under a flow of nitrogen. The reaction was cooled to room temperature and dichloromethane (30 mL) was added to the reaction flask. The solution was filtered over a layer of celite and the solvents then evaporated under reduced pressure. The resulting residue was subjected to purification by silica gel column chromatography with 5% ethyl acetate in hexane to afford **23** as a white solid and **24** as a white solid.

5-(Diphenylmethylene)-3-methylfuran-2(5*H*)-one (23)

Yield: 19%

^{1}H NMR ($CDCl_3$, 400 MHz): 2.02 (3H, d, *J* = 1.4 Hz, C**H$_3$**), 7.09 (1H, q, *J* = 1.4 Hz, **H**-4), 7.25-7.49 (10H, m, **H**-2', **H**-2'', **H**-3', **H**-3'', **H**-4', **H**-4'', **H**-5', **H**-5'', **H**-6', **H**-6''); ^{13}C NMR ($CDCl_3$, 100 MHz): 10.8 (**C**H$_3$) 126.1 (**C**6) 128.2 and 128.4 (**C**2', **C**6', **C**2'', **C**6''') 128.6 and 128.6 (**C**4', **C**4'') 129.1 (**C**3) 131.0 and 131.2 (**C**3', **C**5', **C**3'', **C**5'') 136.8 and 137.6 (**C**1', **C**1'') 138.2 (**C**4) 146.0 (**C**5) 171.4 (**C**2); IR (ATR, cm^{-1}): 3056, 2921, 2851, 1755, 1509, 1444, 1380, 1281, 1250, 1053, 992, 960, 771, 753, 698, 661; HRMS (ESI$^+$): Exact mass calculated for $C_{17}H_{13}O_2^+$ $[M+H]^+$ = 263.1072; Found = 263.1063.

5-(Diphenylmethylene)-4-methylfuran-2(5*H*)-one (24)

Yield: 13%

^{1}H NMR ($CDCl_3$, 400 MHz): 1.54 (3H, d, *J* = 1.2 Hz, C**H$_3$**), 5.99 (1H, q, *J* = 1.2 Hz, **H**-3), 7.26-7.45 (10H, m, **H**-2', **H**-2'', **H**-3', **H**-3'', **H**-4', **H**-4'', **H**-5', **H**-5'', **H**-6', **H**-6''); ^{13}C NMR ($CDCl_3$, 100 MHz) 15.8 (**C**H$_3$), 118.8 (**C**3), 128.1 and 128.6 (**C**2', **C**6', **C**2'', **C**6'''), 128.1 (**C**6), 128.7 and 128.8 (**C**4', **C**4''), 130.8 and 130.9 (**C**3', **C**5', **C**3'', **C**5''), 137.7 and 137.6 (**C**1', **C**1''), 146.7 (**C**4), 156.2 (**C**5), 169.2 (**C**2); IR (ATR, cm^{-1}): 2970, 2927, 1758, 1749, 1592, 1491, 1444, 1323, 1169, 1067, 1054, 959, 738, 699, 632; HRMS (ESI$^+$): Exact mass calculated for $C_{17}H_{13}O_2^+$ $[M+H]^+$ = 263.1072; Found = 263.1062.

Synthesis of methylated furanones 25 and 26

To an oven-dried round bottomed flask was added a mixture of **21/22** (211 mg, 0.787 mmol, 1 eq.), 4-trifluoromethylphenyl boronic acid (448 mg, 2.361 mmol, 3 eq.), tripotassium phosphate (501 mg,

2.361 mmol, 3 eq.), palladium(II) acetate (3 mg, 1 mol%), SPhos (7 mg, 2 mol%) and toluene (5 mL). The reaction mixture was heated to 100 °C for 4 hours under a flow of nitrogen. The reaction was cooled to room temperature and dichloromethane (30 mL) was added to the reaction flask. The solution was filtered over a layer of celite and the solvents then evaporated under reduced pressure. The resulting residue was subjected to purification by silica gel column chromatography with 5% ethyl acetate in hexane to afford **25** as a white solid and **26** as a white solid.

5-(Bis(4-(trifluoromethyl)phenyl)methylene)-3-methylfuran-2(5*H*)-one (25)

Yield: 18%

^{1}H NMR ($CDCl_3$, 400 MHz): 2.06 (3H, d, *J* = 1.3 Hz, C**H$_3$**), 7.07 (1H, q, *J* = 1.3 Hz, **H**-4), 7.39 (2H, d, *J* = 8.1 Hz, **H**-2', **H**-6'), 7.54 (2H, d, *J* = 8.2 Hz, **H**-2'', **H**-6''), 7.61 (2H, d, *J* = 8.2 Hz, **H**-3'', **H**-5''), 7.71 (2H, d, *J* = 8.1 Hz, **H**-3**',** **H**-5'); ^{13}C NMR ($CDCl_3$, 100 MHz): 10.9 (**C**H_3), 123.8 (q, *J* = 272.8 Hz, **C**F_3''), 123.9 (q, *J* = 273.4 Hz, **C**F_3'), 125.3 (q, *J* = 3.7 Hz, **C**3'', **C**5''), 125.7 (q, *J* = 3.6 Hz, **C**3', **C**5'), 130.4 (q, *J* = 32.3 Hz, **C**4''), 130.6 (q, *J* = 32.9 Hz, **C**4'), 131.1 (**C**2'', **C**6''), 131.3 (**C**6), 131.5 (**C**2', **C**6'), 134.7 (**C**3), 137.2 (**C**4), 139.7 (**C**1''), 140.7 (**C**1), 147.4 (**C**5), 170.5 (**C**2); IR (ATR, cm^{-1}): 2925, 2854, 1761, 1614, 1412, 1322, 1127, 1109, 1070, 1048, 993, 967, 846, 755, 567, 476; HRMS (ESI^+): Exact mass calculated for $C_{20}H_{13}F_6O_2^+$ $[M+H]^+$ = 399.0820; Found = 399.0816.

5-(Bis(4-(trifluoromethyl)phenyl)methylene)-4-methylfuran-2(5*H*)-one (26)

Yield: 16%

^{1}H NMR ($CDCl_3$, 300 MHz): 1.58 (3H, d, *J* = 1.2 Hz, C**H$_3$**), 6.10 (1H, q, *J* = 1.2 Hz, **H**-3), 7.43 (2H, d, *J* = 8.0 Hz, **H**-2', **H**-6'), 7.50 (2H, d, *J* = 8.3 Hz, **H**-2'', **H**-6''), 7.59 (2H, d, *J* = 8.3 Hz, **H**-3'', **H**-5''), 7.73 (2H, d, *J* = 8.0 Hz, **H**-3', **H**-5'); ^{13}C NMR ($CDCl_3$, 75.5 MHz): 15.9 (**C**H_3), 120.3 (**C**3), 124.4 (**C**6), 123.8 (q, *J* = 272.7 Hz, **C**F_3'), 123.7 (q, *J* = 272.7 Hz, **C**F_3''), 125.8 (q, *J* = 3.7 Hz, **C**3', **C**5'), 125.2 (*J* = 3.7 Hz, **C**3'', **C**5''), 130.5 (q, *J* = 32.7 Hz, **C**4''), 131.5 (q, *J* = 32.8 Hz, **C**4'), 130.9 (**C**2'', **C**6''), 131.2 (**C**2', **C**6'), 140.4 (**C**1', **C**1''), 147.9 (**C**4), 155.3 (**C**5), 168.1 (**C**2); IR (ATR, cm^{-1}): 2918, 1775, 1755, 1615, 1600, 1575, 1385, 1318, 1163, 1116, 1107, 1065, 964, 882, 729, 639, 495; HRMS (ESI^+) Exact mass calculated for $C_{20}H_{13}F_6O_2^+$ $[M+H]^+$ = 399.0820; Found = 399.0825

Synthesis of 5-(bis(4-fluorophenyl)methylene)-3-bromofuran-2(5*H*)-one (29)

To a stirred solution of **15** (82 mg, 0.288 mmol) in chloroform (0.5 mL) was slowly added a solution of bromine (0.014 mL, 0.286 mmol) in chloroform (0.5 mL). The reaction mixture was heated to reflux for 4 hours, after which time the mixture was sparged with nitrogen for 10 minutes to remove excess bromine. The resulting solution was then cooled to 0°C and a solution of trimethylamine (0.079 mL, 0.572 mmol) in chloroform (0.25 mL) was added dropwise over 10 minutes. The reaction was stirred for an additional hour at 0°C before the reaction was allowed to reach room temperature. The reaction solution was washed with water (3 x 15 mL) and brine (15 mL) and then

dried over anhydrous magnesium sulfate. The solvent was removed under reduced pressure and crude reaction mixture was purified *via* silica gel column chromatography with 5%-10% ethyl acetate in hexane to afford **29** as a yellow solid.

Yield: 82%

^{1}H NMR ($CDCl_3$, 400 MHz): 7.03-7.09 (2H, m, **H**-3'', **H**-5''), 7.12-7.18 (2H, m, **H**-3', **H**-5'), 7.23-7.28 (2H, m, **H**-2', **H**-6'), 7.43-7.47 (2H, m, **H**-2'', **H**-6''), 7.48 (1H, s, **H**-4); ^{13}C NMR ($CDCl_3$, 75.5 MHz): 112.2 (**C**6), 115.7 (d, *J* = 37.0, **C**3'', **C**5''), 115.9 (d, *J* = 37.1, **C**3', **C**5'), 127.2 (**C**3), 132.0 (d, *J* = 3.4 Hz, **C**1'), 132.6 (d, *J* = 3.4 Hz, **C**1''), 132.8 (d, *J* = 8.4 Hz, **C**2', **C**6'), 133.2 (d, *J* = 8.2 Hz, **C**2'', **C**6''), 141.4 (**C**4) 145.3 (**C**5) 163.2 (d, *J* – 251.8 Hz, **C**4''), 163.3 (d, *J* = 252.5 Hz, **C**4'), 165.7 (**C**2); IR (ATR, cm^{-1}): 2924, 1790, 1770, 1600, 1506, 1409, 1228, 1159, 1175.1159, 980, 837, 738, 731, 590, 547; HRMS (ESI^+): Exact mass calculated for $C_{17}H_{10}{}^{79}BrF_2O_2^+$ $[M+H]^+$ = 362.9832; Found = 362.9816.

Synthesis of 5-(pentadeca-6,9-diyn-8-ylidene)furan-2(5*H*)-one (31)

gem-Dibromofuranone **4** (300 mg, 1.181 mmol), triphenylphosphine (62 mg, 20 mol%), bis(triphenylphosphine)palladium(II) dichloride (83 mg, 10 mol%) and copper(I) iodide (45 mg, 20 mol%) were added to an oven dried round bottomed flask under a flow of nitrogen. Diisopropylamine (5 mL) and 1-heptyne (0.341 mL, 2.599 mmol) were subsequently added to the reaction flask. The mixture was stirred at room temperature for 24 hours after which time the reaction was quenched with saturated aqueous ammonium chloride solution. The mixture was extracted with dichloromethane (3 x 30 mL) and the combined organic layers were washed with water (3 x 30 mL) and brine (3 x 30 mL), dried with anhydrous magnesium sulfate and concentrated under reduced pressure. The crude product was purified by silica gel column chromatography with 5%-10% ethyl acetate in hexane to afford **31** as a dark orange oil.

Yield: 63%

^{1}H NMR ($CDCl_3$, 400 MHz): 0.88-0.94 (6H, m, $\mathbf{H_3}$-15', $\mathbf{H_3}$-1'), 1.28-1.45 (8H, m, $\mathbf{H_2}$-13', $\mathbf{H_2}$-3', $\mathbf{H_2}$-14', $\mathbf{H_2}$-2'), 1.55-1.61 (4H, m, $\mathbf{H_2}$-12', $\mathbf{H_2}$-4'), 2.36-2.44 (4H, m, $\mathbf{H_2}$-11', $\mathbf{H_2}$-5'), 6.20 (1H, d, *J* = 5.4 Hz, **H**-3), 7.70 (1H, d, *J* = 5. Hz, **H**-4); ^{13}C NMR ($CDCl_3$, 75.5 MHz): 13.9 (**C**15', **C**1'), 19.6 and 20.0 (**C**11', **C**5'), 22.12 and 22.14 (**C**14', **C**2'), 27.9 and 28.0 (**C**12', **C**4'), 31.07 and 31.10 (**C**13', **C**3'), 74.7 and 75.0 (**C**9', **C**7'), 92.9 (**C**8'), 96.7 and 102.4 (**C**6', **C**10''), 119.7 (**C**3), 140.5 (**C**4), 159.0 (**C**5), 168.6 (**C**2); IR (ATR, cm^{-1}): 2955, 2929, 2859, 2214, 1779, 1603, 1541, 1510, 1465, 1378, 1327, 1242, 1103, 953, 880, 812, 727, 710, 542; HRMS (ESI^+): Exact mass calculated for $C_{19}H_{25}O_2^+$ $[M+H]^+$ = 285.1855; Found = 285.1844.

Synthesis of 5-(heptadeca-7,10-diyn-9-ylidene)furan-2(5*H*)-one (32)

gem-Dibromofuranone **4** (300 mg, 1.181 mmol), triphenylphosphine (62 mg, 20 mol%), bis(triphenylphosphine)palladium(II) dichloride (83 mg, 10 mol%) and copper(I) iodide (45 mg, 20

mol%) were added to an oven dried round bottomed flask under a flow of nitrogen. Diisopropylamine (5 mL) and 1-octyne (0.431 mL, 2.596 mmol) were subsequently added to the reaction flask. The mixture was stirred at room temperature for 24 hours after which time the reaction was quenched with saturated aqueous ammonium chloride solution. The mixture was extracted with dichloromethane (3 x 30 mL) and the combined organic layers were washed with water (3 x 30 mL) and brine (3 x 30 mL), dried with anhydrous magnesium sulfate and concentrated under reduced pressure. The crude product was purified by silica gel column chromatography with 5%-10% ethyl acetate in hexane to afford **32** as an orange oil.

Yield: 41%

^{1}H NMR ($CDCl_3$, 400 MHz): 0.86-0.93 (6H, m, $\mathbf{H_3}$-17', $\mathbf{H_3}$-1'), 1.24-1.36 (8H, m, $\mathbf{H_2}$-15', $\mathbf{H_2}$-3', $\mathbf{H_2}$-16', $\mathbf{H_2}$-2'), 1.37-1.47 (4H, m, $\mathbf{H_2}$-14', $\mathbf{H_2}$-4'), 1.54-1.64 (4H, m, $\mathbf{H_2}$-13', $\mathbf{H_2}$-5'), 2.37-2.46 (4H, m, $\mathbf{H_2}$-12', $\mathbf{H_2}$-6'), 6.21 (1H, d, *J* = 5.4 Hz, **H**-3), 7.70 (1H, d, *J* = 5.4 Hz, **H**-4); ^{13}C NMR ($CDCl_3$, 100 MHz): 14.1 (**C**17', **C**1'), 19.7 and 20.1 (**C**12', **C**6'), 22.5 and 22.5 (**C**16', **C**2'), 28.2 and 28.3 (**C**13', **C**5'), 28.6 and 28.6 (**C**14', **C**4'), 31.27 and 31.29 (**C**15', **C**3'), 74.7 and 75.0 (**C**10', **C**8'), 92.9 (**C**9'), 96.7 and 102.4 (**C**11', **C**7'), 119.7 (**C**3), 140.5 (**C**4), 159.0 (**C**5), 168.7 (**C**2); IR (ATR, cm^{-1}): 2954, 2927, 2857, 2214, 1781, 1747, 1714, 1627, 1542, 1458, 1400, 1378, 1124, 1176, 1143, 1105, 1060, 1032, 972, 818, 724, 699, 466, 438, 417, 4088; HRMS (ESI$^+$): Exact mass calculated for $C_{21}H_{29}O_2^+$ $[M+H]^+$ = 313.2168; Found = 313.2161.

Synthesis of (*Z*)-5-(chloro(4-nitrophenyl)methylene)furan-2(5*H*)-one (38)

34 (45 mg, 0.272 mmol), 4-nitrophenyl boronic acid (50 mg, 0.299 mmol), tripotassium phosphate (115 mg, 0.544 mmol), palladium(II) acetate (2 mg, 3 mol%), SPhos (2.2 mg, 2 mol%) and toluene (1 mL) were added to a round bottomed flask under a flow of nitrogen. The reaction mixture was stirred at room temperature for 48 hours and then diluted with dichloromethane (10 mL). The crude reaction mixture was filtered over a layer of Celite and the solvent evaporated under reduced pressure. The crude product was purified *via* silica gel column chromatography with 5%-10% ethyl acetate in hexane to afford **38** as a white solid.

Yield: 52%

^{1}H NMR ($CDCl_3$, 400 MHz): 6.40 (1H, d, *J* = 5.6 Hz, **H**-3), 7.49 (1H, d, *J* = 5.6 Hz, **H**-4), 7.70 (2H, td, *J* = 8.9 Hz, 2.4 Hz, **H**-2', **H**-6'), 8.33 (2H, td, *J* = 8.9 Hz, 2.4 Hz, **H**-3', **H**-5'); ^{13}C NMR ($CDCl_3$, 100 MHz): 117.2 (**C**Cl), 122.1 (**C**3), 124.1 (**C**3', **C**5'), 130.5 (**C**2', **C**6'), 140.2 (**C**1'), 140.5 (**C**4), 148.6 (**C**5), 148.6 (**C**NO_2), 167.6 (**C**2); IR (ATR, cm^{-1}): 3109, 2923, 1778, 1747, 1596, 1521, 1348, 1235, 1110, 1075, 962, 942, 861, 850, 812, 751, 693, 470; HRMS (ESI$^+$) Exact mass calculated for $C_{11}H_7{}^{35}ClNO_4^+$ $[M+H]^+$ = 252.0064; Found = 252.0055.

Synthesis of methyl *N*-(*tert*-butoxycarbonyl)-*S*-((2-(dibromomethylene)-5-oxo-2,5-dihydrofuran-3-yl)methyl)cysteinate (41)

To a solution of *tert*-butoxycarbonyl-cysteine methyl ester (272 mg, 1.156 mmol) in tetrahydrofuran (22 mL) was added triethylamine (0.485 mL, 3.477 mmol) and allylic bromide **39** (402 mg, 1.159 mmol). After stirring at 80°C for 4 hours under a nitrogen atmosphere, the solvents were evaporated under reduced pressure. Purification *via* silica gel column chromatography with 20% ethyl acetate in hexane furnished **41** as an off-white solid.

Yield: 43%

^{1}H NMR ($CDCl_3$, 300 MHz): 1.45 (9H, s, (C**H$_3$**)$_3$), 2.86-3.06 (2H, m, SC**H$_2$**CHNH), 3.79 (3H, s, OC**H$_3$**), 3.87 (2H, d, *J* = 1.1 Hz, C**H$_2$**SCH_2), 4.55 (1H, m, C**H**NH), 5.35 (1H, d, *J* = 5.7 Hz, N**H**), 6.42 (1H, t, *J* = 1.1 Hz, **H**-4); ^{13}C NMR ($CDCl_3$, 75.5 MHz): 28.3 (**C**H_3)$_3$), 29.8 (**C**H_2SCH_2), 33.8 (SCH_2C**H**NH), 52.9 (O**C**H_3), 53.4 (**C**HNH), 80.6 (**C**$(CH_3)_3$), 81.2 (**C**Br_2), 121.4 (**C**4), 148.5 (**C**=CBr_2), 152.8 (**C**3), 155.0 (**C**OONH), 165.0 (**C**5), 171.0 (**C**OOCH_3); IR (ATR, cm^{-1}): 3364, 2978, 2929, 2850, 1773, 1746, 1704, 1588, 1511, 1504, 1344, 1217, 1159, 1045, 952, 849, 713, 640; HRMS (ESI$^+$): Exact mass calculated for $NaC_{15}H_{19}{}^{79}Br_2NO_6S$ [M+Na]$^+$ = 521.9198; Found = 521.9173.

Microbial analysis

***V. harveyi* and *E. coli* growth and quorum sensing inhibition assay**

V. harveyi BB120, *V. harveyi* BB170, *V. harveyi* BB152 and *E. coli* pPL2-*lux*P_{HELP} (constitutively expressing *lux*) were routinely cultured aerobically in Marine Broth (Difco) for *V. harveyi* and LB media for *E. coli* at 30 °C with shaking, and Marine Broth- and LB-agar plates were used for growth on solid media [32]. To test the effect of the furanones on bacterial growth, QS systems or impact upon constitutive lux expression bacteria were grown to the exponential phase (OD_{600nm} 1) and pelleted at 6000 g for 3 minutes. The pellet was first washed two times in phosphate buffered saline (PBS, Sigma-Aldrich) and washed one time in Marine Broth or LB. Bacteria were resuspended in broth media or broth media supplemented with 1 µM or 10 µM of a furanone at an initial of OD_{600nm} 0.1 and transferred into two separate flat-bottom 96-well microplates (Costar), at a volume of 200 µL per well in duplicates or triplicates. Marine or LB Broth was used for blank measurements. The plates were incubated at 30 °C for 2 hours and growth of *V. harveyi* and *E. coli* was analysed through measurements of OD_{600nm} on a plate reader (Tecan Sunrise). Simultaneously, the activation levels of the Lux QS and the constitutively active *lux*P_{HELP} were monitored by bioluminescence measurements as flux (photon/second) in an IVIS Spectrum System (Perkin Elmer). Relative growth and relative bioluminescence were calculated as a normalization to the control condition (*V. harveyi* in Marine Broth as 100%). The assays were performed in duplicate or triplicate. All furanones were screened against wild-type *V. harveyi* BB120, with selected compounds also tested in identical assays using *V. harveyi* BB170 (*luxN*::Tn5) (sensor 1$^-$, sensor 2$^+$) which does not detect AI-1 and *V. harveyi* BB152 (*luxL*::Tn5) (AI-1$^-$, AI-2$^+$) which does not produce AI-1 [33].

Results and discussion

Chemistry

Maleic anhydride (**5**) was initially subjected to Ramirez olefination to generate *gem*-dibromofuranone **4** which served a common precursor for a library of aryl-substituted derivatives (Figure 2A). These derivatives (**6**-**19**) were prepared *via* Suzuki coupling to the appropriate boronic acid as previously reported [31, 34]. Room temperature reaction with one equivalent of boronic acid led the formation of monoarylated furanones (i.e. **6**,**8**,**10**,**12**,**14**,**17**,**18**) all with *Z*-configuration. Repeating the reaction at 100 °C with three equivalents favoured formation of the diarylated furanones (i.e. **7**,**9**,**11**,**13**,**15**,**16**,**19**).

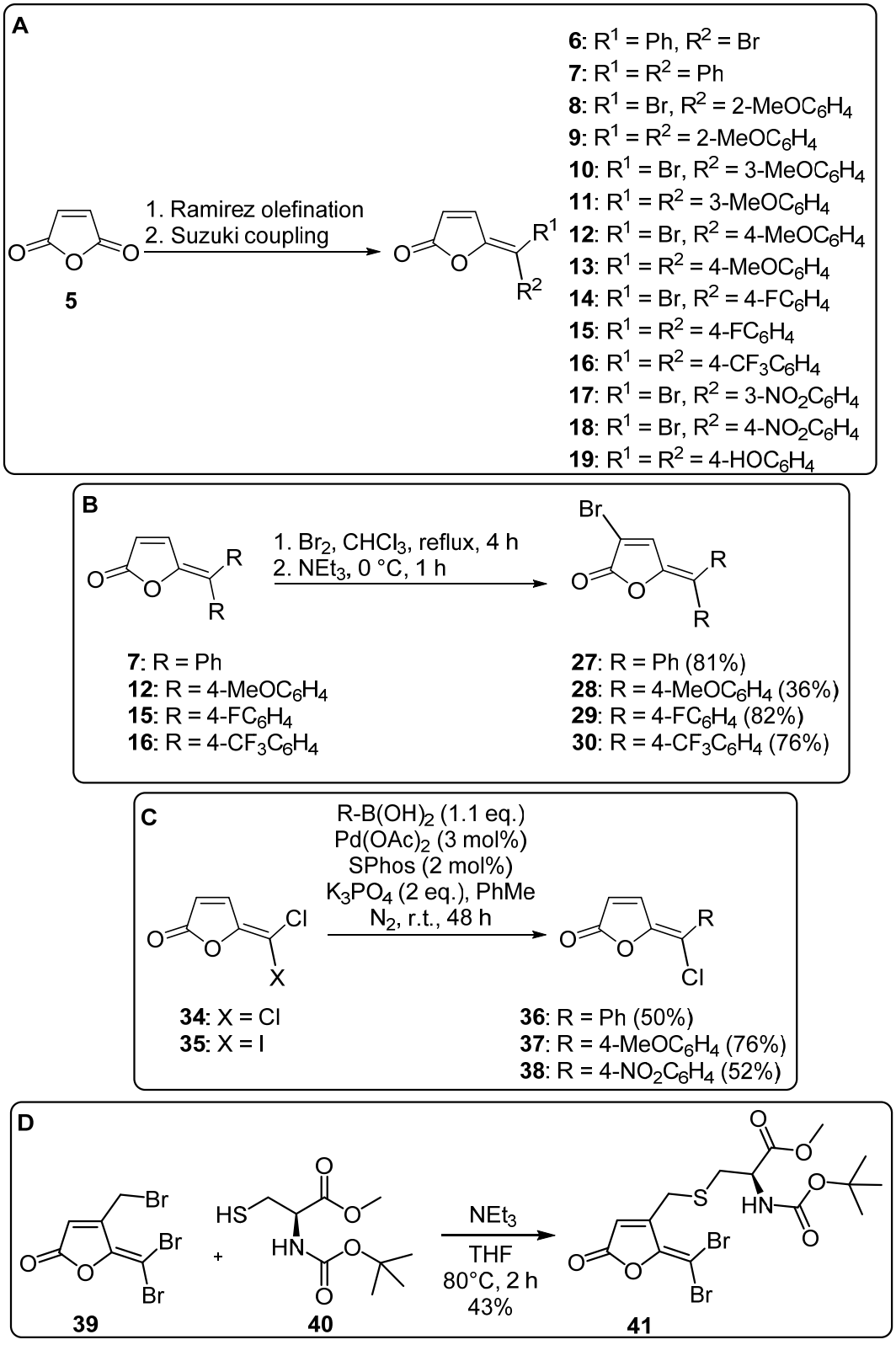

Figure 2. Furanone synthesis. (A) Generation of aryl-substituted furanones. **(B)** Regioselective bromination of *gem*-diarylated furanones. **(C)** Chlorine- and iodine-containing furanones. **(D)** Incorporation of cysteine sidechain.

The incorporation of a 3- or 4-alkyl group into the furanone ring has been linked to reduced toxicity [35, 36]. Accordingly, dibromoolefination of methylsuccinic anhydride (**20**) afforded a mixture of regioisomeric products, namely 3-methyl-substituted *gem*-dibromofuranone **21** and 4-methyl-substituted **22** (Table 1). Due to the difficulties in separating the isomeric mixture, **21** and **22** were directly subjected to Suzuki coupling with an excess of phenyl boronic acid at 100 °C using SPhos as the ligand. These conditions furnished the corresponding 3- and 4-methyl *gem*-diphenylfuranone analogues **23** (entry 1) and **24** (entry 2) respectively. This approach was repeated with 4-trifluoromethylphenyl boronic acid to afford novel *gem*-diarylfuranones **25** (entry 3) and **26** (entry 4) in a similar fashion. Not unexpectedly, the products has similar polarities and proved challenging to separate, which impacted negatively on isolated yields (entries 1-4).

Table 1. Preparation of 3- and 4-methylated furanones.

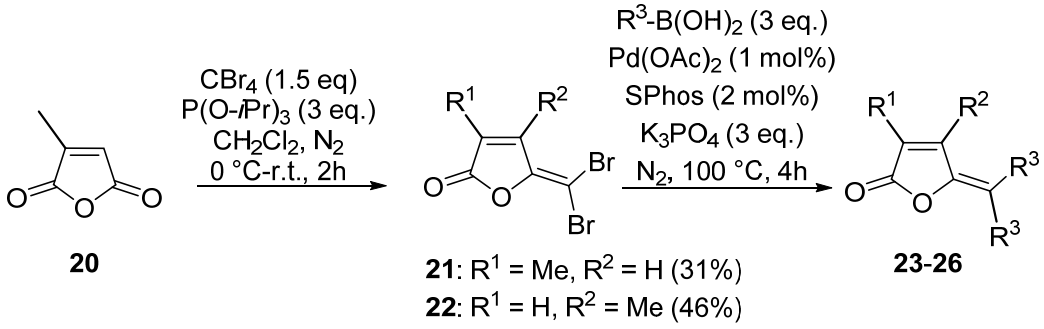

Entry	R^1	R^2	R^3	Product	Yield
1	Me	H	Ph	**23**	19%
2	H	Me	Ph	**24**	13%
3	Me	H	4-$CF_3C_6H_4$	**25**	18%
4	H	Me	4-$CF_3C_6H_4$	**26**	16%

Several groups have noted how the presence of a bromine atom at the C3 or C4 positions can give rise to more effective QS inhibitors [35-37]. Bromination of several *gem*-diarylated furanones proceeded smoothly to afford the 3-brominated products (Figure 2B). Taking 4-fluorophenyl-substituted furanone **15** as an example, heating of **15** to reflux in the presence of bromine, followed by addition of triethylamine at 0 °C, afforded novel 3-brominated furanone **29** in 82% yield. These reactions were all found to be regioselective, with none of the 4-brominated isomers being detected.

Kumar and colleagues previously tested a series of alkyne-containing furanones against the *P. aeruginosa* MH602 *lasB* reporter strain and identified several active compounds with favourable toxicity profiles [38]. A Pd/Cu-mediated coupling of **4** with an excess of 1-heptyne at room temperature produced diheptynyl-substituted **31** in 63% yield (Table 2, entry 1). As some literature precedent suggests that longer alkyl chains can confer reduced toxicity [39, 40], a similar Sonagashira reaction was conducted with 1-octyne. Homologue **32** was subsequently isolated in 41% yield (entry 2). Coupling of **4** with an aromatic substrate required more forcing conditions and higher temperatures (entry 3).

Table 2. Synthesis of alkyne-containing analogues *via* Sonogashira coupling.

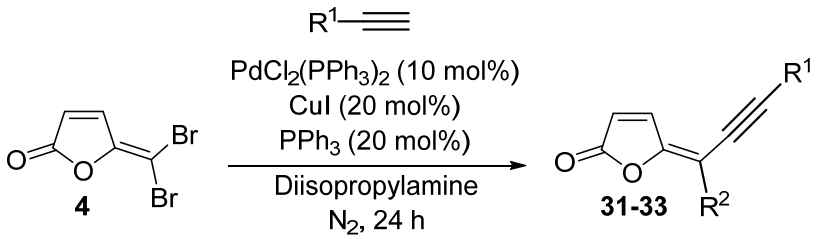

Entry	R^1	Equiv.	Temp.	Product	R^2	Yield
1	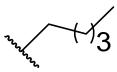	2.1	r.t.	**31**		63%
2	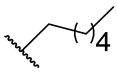	2.1	r.t.	**32**		41%
3	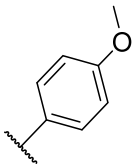	2.2	80 °C	**33**	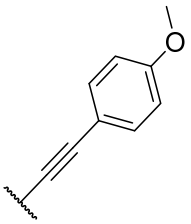	34%

In addition to *gem*-dibromofuranone derivatives, *gem*-dichloroolefin **34** and *gem*-chloroiodoolefin **35** were also evaluated in this study (Figure 2C) [34]. **34** also served as a common precursor for a series of furanone derivatives **36**-**38**. Accordingly, palladium-mediated coupling of **34** with 1.1

equivalents of 4-nitrophenyl boronic acid at room temperature provided monoarylated product **38** in a yield of 52%. In each case, **36**, **37** and **38** were isolated as their *Z*-isomers exclusively.

Analogues of *S*-ribosylhomocysteine have recently attracted attention as potential quorum sensing inhibitors [41-43]. Evidence exists to suggest that brominated furanones inactivate the enzyme which converts *S*-ribosylhomocysteine into homocysteine [24]. With that in mind, we wondered whether incorporation of a homocysteine-like sidechain might provide a better fit for the enzyme active site. Adapting a procedure of Li and colleagues [44], addition of three equivalents of triethylamine to **39** and *tert*-butoxycarbonyl-protected cysteine **40** saw partial conversion to **41** over 16 hours (Figure 2D). Increasing the reaction temperature to 80°C saw complete conversion of **39** to **41** after only 2 hours, with **41** recovered in a yield of 43% following purification. Subsequent attempts at cleaving the *N*-*tert*-butoxycarbonyl protecting group or hydrolysis of the methyl ester resulted solely in degradation of **41**, so the diester was instead assayed for activity.

Evaluation of furanone library

The normalised percentage growth of *V. harveyi* BB120 in the presence of our furanones was measured after two hours (Figure 3A). The majority of compounds had a negligible effect on bacterial growth at either 1 μM or 10 μM concentrations. This is important as it suggests that any subsequent effects on bioluminescence can be attributed to quorum sensing inhibition or other effects upon bacterial physiology. 4-Methyl-substituted dibromofuranone **22** had the largest inhibitory effect on *V. harveyi* growth, with a reduction of 21% recorded. Interestingly, its corresponding isomer, namely 3-methylsubstituted **21**, reduced growth by a mere 3%. Tribromofuranone **39**, a close analogue of **22**, caused a smaller reduction of 15%. Of the remaining compounds, two chlorine-containing furanones proved to have the greatest effect. Chloroiodofuranone **35** and 4-nitrophenylchlorofuranone **38** inhibited cell growth by 19% and 20% respectively at 10 μM concentration. Only one compound had an inhibitory effect at 1 μM concentration i.e. chloroiodofuranone **35**. **35** proved almost equipotent at the lower concentration and retarded growth by 19%.

A

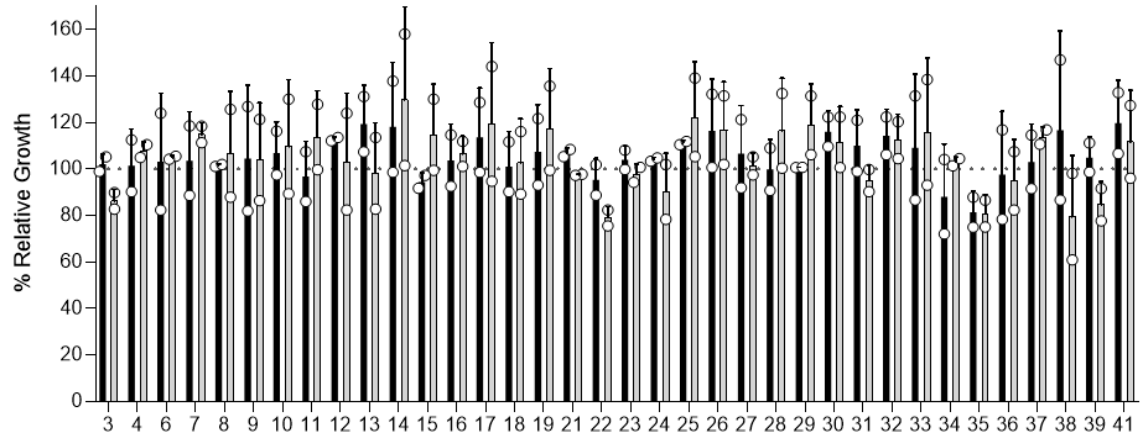

B

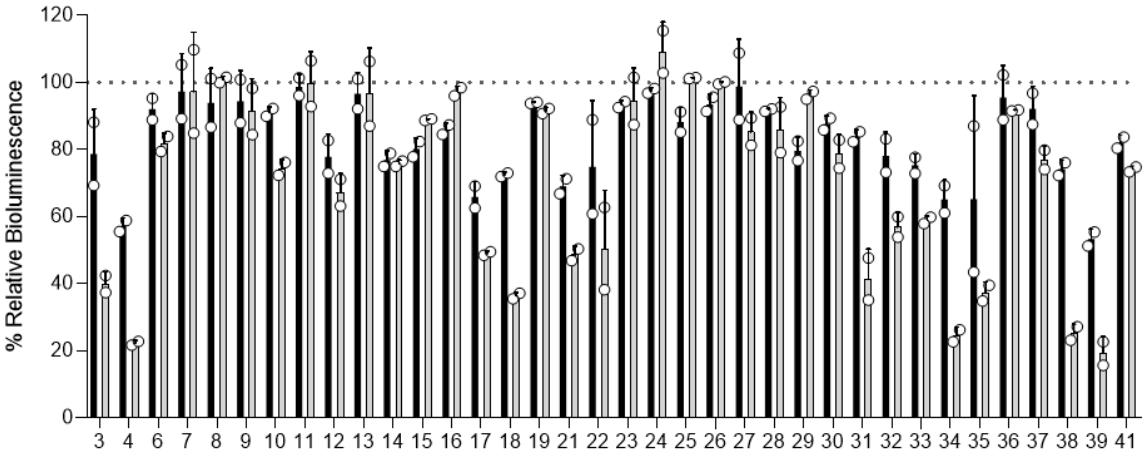

Figure 3. Evaluation of furanone library. (A) Effect of furanones on the growth of *V. harveyi* BB120. Relative growth in the presence of 1 μM or 10 μM of furanones is represented as percentage of the control condition (*V. harveyi* BB120 in Marine Broth as 100%). Data is represented as vertical bars and error bars as mean data and associated standard deviation, with scatterplot overlay of individual datapoints. **(B)** Effect of furanones on the bioluminescence of *V. harveyi* BB120 as an index of potential effects on the QS system. Relative bioluminescense in the presence of 1 μM or 10 μM of furanones is represented as percentage of the control condition (*V. harveyi* BB120 in Marine Broth as 100%). Data is represented as vertical bars and error bars as mean data and associated standard deviation, with scatterplot overlay of individual datapoints. The dark bars represent the effects of the 1 μM concentration and the light grey bars represent 10 μM concentrations of the individual compounds screened. The individual white circles represent the duplicate readings at each concentration.

The same library of furanones was next tested for potential to inhibit the QS system of *V. harveyi* BB120 as measured by bioluminescence imaging (Figure 3B). Inhibition readings were taken after

incubating *V. harveyi* BB120 with the appropriate furanones for two hours. *V. harveyi* BB120 can produce and detect AI-2, HAI-1 and CAI-1. As bioluminescence readings were taken when the bacteria were in the exponential phase of growth (i.e., when CAI-1 is not detectable), bioluminescence can broadly be attributed to HAI-1 and AI-2. It is worth noting that HAI-1 is present at low levels during this phase of growth. Bioluminescence without the addition of our furanones was set to 100% (control) and other samples were normalised accordingly. Two replicates of each experiment were performed in this screen to determine error bars and reproducibility (individual datapoints are shown).

Tribromofuranone **39** was the most active compound inhibiting bioluminescence by 81% at 10 μM concentration. We have previously noted that this compound is a highly effective biofilm inhibitor of *S. enterica*, *S. aureus* and *P. aeruginosa* [31]. While known dibromofuranone **4** inhibited bioluminescence by 77%, the corresponding 3-methyl- and 4-methyl-substituted derivatives **21** and **22** were less active and reduced bioluminescence by only 50%. The presence of a bromine atom was not a prerequisite for activity. Chloroiodofuranone **35** proved to be a potent inhibitor of *V. harveyi* bioluminescence with 63% inhibition recorded. In comparison, dichlorofuranone **34** was even more efficacious and reduced bioluminescence by 74%.

The incorporation of an aryl ring *via* Suzuki coupling generated compounds with lower inhibitory activity. Phenyl-substituted bromofuranone **6** was slightly more active than corresponding chlorofuranone **36**, reducing bioluminescence by 19% and 9% respectively. The corresponding diphenyl-substituted analogue **7** was essentially inactive. The presence of a methyl group on the furanone ring in the case of **23** and **24** was not associated with increased QS inhibition. A small increase in activity was observed when bromine was incorporated into the furanone ring at C3, with a 15% reduction in bioluminescence recorded for **27**. The introduction of substituents to the aryl rings did impact on biological activity and was dependent on both the nature of the substituent and the substitution pattern. For example, 4-methoxyphenyl-substituted furanone **12** inhibited bioluminescence by 33%. By comparison, 3-methoxyphenyl-substituted **10** was slightly less potent at 26% inhibition, while 2-methoxyphenyl-substituted **8** had no inhibitory effect. The corresponding diarylated analogues **13**, **11** and **9** were inactive. 4-Methoxyphenyl-substituted chlorofuranone **37** was a less effective inhibitor than its bromine-containing counterpart **12**, reducing bioluminescence by 23%.

Nitrophenyl-substituted bromofuranones **17** and **18** were found to be two of the most active compounds. 4-Nitrophenyl-substituted analogue **18** inhibited bioluminescence by 65% at 10 μM concentration. 3-Nitrophenyl-substituted analogue **17** was slightly less active and saw a 50% reduction in bioluminescence. Importantly, neither analogue inhibited the growth of *V. harveyi*.

Novel chlorine-containing 4-nitrophenyl-substituted **38** was the most potent compound in this series with 73% anti-bioluminescence activity recorded. Replacing the nitro group with a fluorine atom proved detrimental with 4-fluorophenyl-substituted bromofuranone **14** causing 25% inhibition. Its corresponding diarylated equivalent **15**, which lacks an exocyclic bromine, was less active (11% reduction), while the corresponding 4-trifluoromethyl-substituted analogue **16** was essentially inactive.

Several antimicrobial natural products contain alkyne motifs, including falcarindiol [45], dragomabin [46] and the calicheamicins [47]. Sonogashira chemistry provided ready access to a series of alkyne-containing furanones which were evaluated against *V. harveyi* BB120. At 10 μM concentration, heptyne-substituted **31** was found to inhibit bioluminescence by 52%. Increasing the length of the alkyl chain had a negative impact with a 40% reduction in bioluminescence observed for **32**. Replacing the alkyl chain with an aromatic ring in **33** afforded an equipotent compound (42% inhibition). All of the dialkynyl-containing furanones had a negligible effect on bacterial growth (Figure 2A).

Lastly, a *gem*-dibromofuranone-cysteine conjugate was investigated as a potential QS inhibitor. Conjugate **41** proved biologically active and inhibited bioluminescence by 27%. Additionally, **41** did not affect bacterial growth. Overall, however, **41** was less promising than other candidates described above.

Given the experimental design, the effects of individual compounds on bioluminescence in wild-type *V. harveyi* BB120 most likely reflect their impact on AI-2 signalling. To further verify this, we analysed the effects of three molecules (bromofuranones **3**, **4** and dichlorofuranone **34**) on bioluminescence signalling in engineered reporter strains (*V. harveyi* BB152 (which lacks production of AI-1) and V*. harveyi* BB170 (which lacks the ability to detect AI-1) [33]. Both of the engineered reporter strains have intact AI-2 systems but deficits in AI-1. The data confirm that the compounds do not affect bacterial growth of any of the three strains (Figure 4). When we examined bioluminescence in the absence of AI-1 signalling, it was reduced by all three furnanones strongly suggesting that the compounds impact AI-2 production or AI-2 signalling events (Figure 5). This finding is especially notable for **34** as *gem*-dichlorofuranones have not been widely investigated as potential inhibitors of AI-2 quorum sensing.

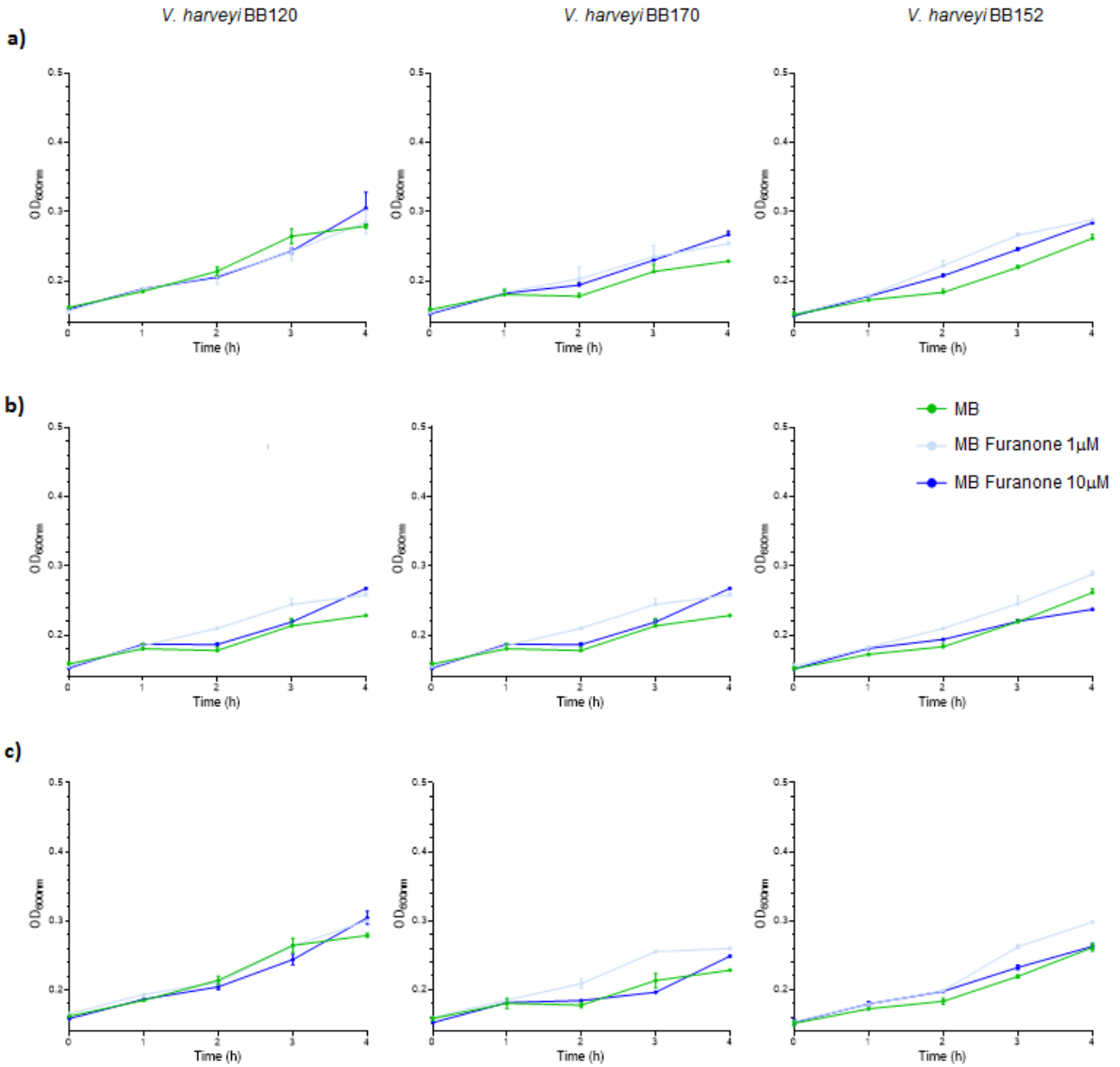

Figure 4. Furanones 3, 4 and 34 do not affect growth of *V. harveyi.* Growth (OD_{600nm}) of *V. harveyi* BB120, *V. harveyi* BB170 and *V. harveyi* BB152 in the presence of 1 µM or 10 µM of **a)** furanone **3**, **b)** furanone **4** and **c)** furanone **34**. Data is represented as mean and associated standard deviation.

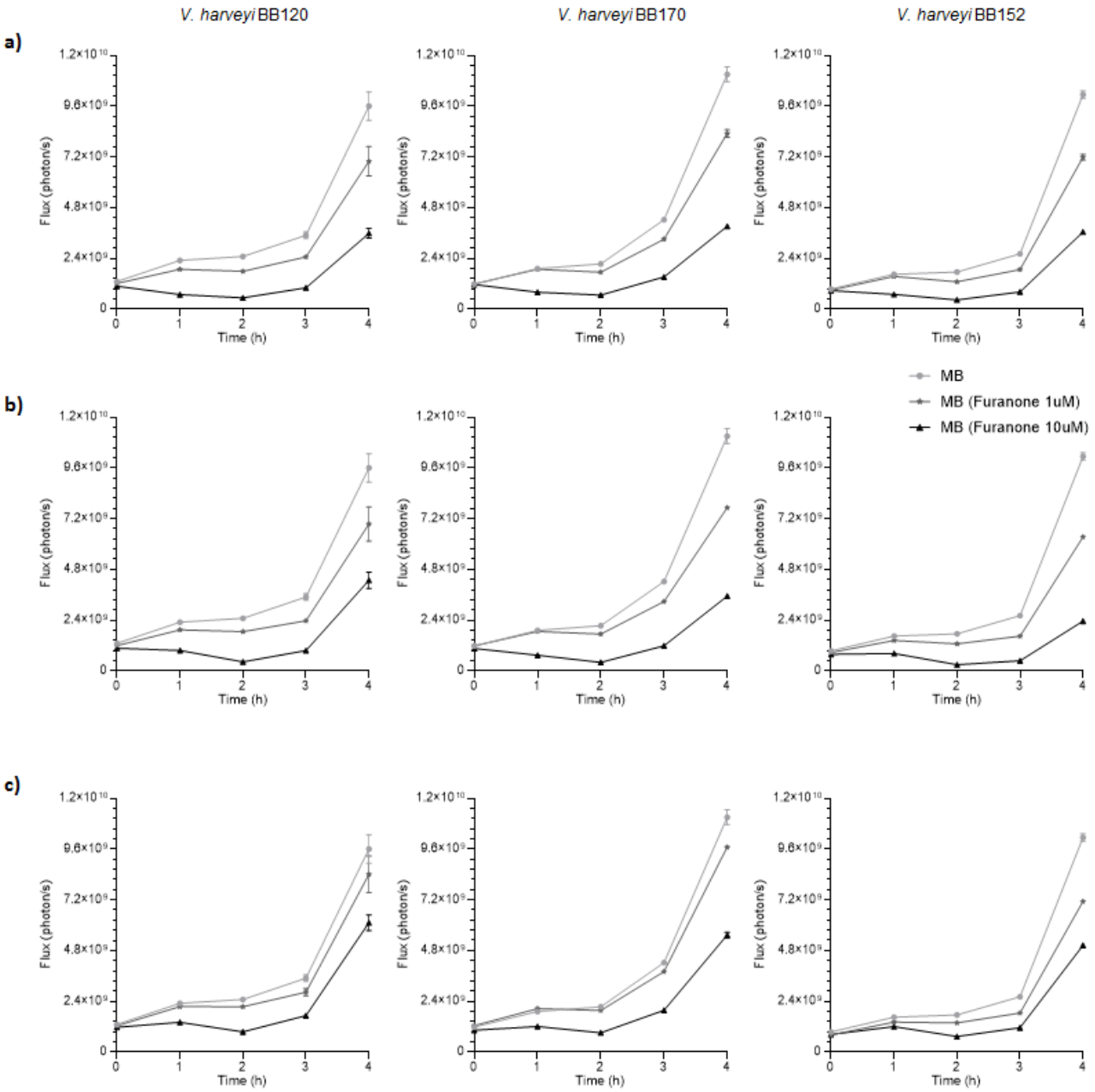

Figure 5. Furanones 3, 4 and 34 inhibit the QS system of *V. harveyi* strains. Bioluminescence (Flux) from *V. harveyi* BB120, *V. harveyi* BB170 and *V. harveyi* BB152 in the presence of 1 μM or 10 μM of **a)** furanone **3**, **b)** furanone **4** and **c)** furanone **34**. Data is represented as mean and associated standard deviation.

From the library of compounds assayed, the most potent typically contained vinylic bromines, such as tribromofuranone **39** and nitrophenyl-substituted bromofuranones **17** and **18**. These results are unsurprising and align with several previous studies [27]. Brominated furanones can covalently bind to nucleophilic residues (e.g. cysteine or histidine) at the LuxS active site *via* an addition-elimination mechanism [24]. This inactivates the enzyme as it is unable to bind its substrate, namely *S*-

ribosylhomocysteine. The inability of the LuxS substrate to bind to the active site inhibits the synthesis of AI-2 and should, in theory, block bioluminescence, biofilm formation and toxin production. In the case of **39**, the additional bromine atom on the side chain is even more susceptible to nucleophilic substitution [36]. However, several other potential bioluminescence inhibitors were also identified which did not follow this trend. These included *gem*-dichlorofuranone **34**, 4-nitrophenyl-substituted chlorofuranone **38** and chloroiodofuranone **35**. Chlorinated furanones have received little attention as possible QS inhibitors until now. Although tribromofuranone **39** was the most potent compound in this study, the negligible effects of **17**, **18** or **34** on *V. harveyi* growth points to their greater potential as QS inhibitors which do not exert selective pressure for resistance. Alkyne derivatives **31** and **32** may likewise warrant further investigation given their benign impact on cell growth.

In an effort to better characterise the biological activities of the active compounds, we determined that **3**, **4** and **34** affected growth of an *E. coli* strain in which a plasmid-borne *lux* operon is constitutively expressed, thereby suggesting species-specific effects upon growth. Interestingly, furanone **3** inhibited bioluminescence in the *E. coli* control suggesting non-specific activity of this compound on the bioluminescence signal, whereas dichlorofuranone **34** did not exhibit this non-specific effect (Supplementary Figure 1). Future work from our group will examine the specific role of our furanones on QS signalling, biofilm formation and bacterial physiology.

Each of the furanones was also screened *in silico* using the SwissADME website to assess their physicochemical properties and suitability for further development [48]. Among the properties calculated include molecular weight, number of hydrogen bond acceptors or donors, and cLog P (Table 3). In conjunction with Lipinski's rule of five, these parameters may be used to identify molecules with poor absorption or permeation characteristics meaning they are less likely to be orally active [49]. Gratifyingly, none of the furanones screened was found to violate two or more of Lipinski's requirements. A small number of compounds (i.e. **16**, **25**, **26**, **29**, **30**) did violate one requirement and this was primarily associated with cLog P values above five. In each case, the high lipophilicity can be accounted for by the presence of fluorine in their structures. Additionally, one other compound (i.e. **41**) had a molecular weight greater than 500.

Veber's rule uses an alternate set of criteria to evaluate the suitability of a drug candidate for oral drug delivery [50]. It requires that the topological polar surface area (TPSA) of the molecule should be under 140 $Å^2$, the total number of rotatable bonds should be under 10 and that the total number of H-bonds (i.e. sum of hydrogen bond acceptors (HBA) and donors (HBD)) should be under 12. The strength of Veber's rule derives from the observation that polar surface area correlates better

with permeability than lipophilicity, while the number of rotatable bonds impacts negatively on permeation. All of the compounds in this study were found to fall within acceptable limits (Table 3).

Table 3. Screening *in silico* using Lipinski's and Veber's rules.

Furanone	MW	HBA	HBD	cLog P	TPSA ($Å^2$)	Rotatable Bonds	HBA+HBD
3	174.98	2	0	1.29	26.3	0	2
4	253.88	2	0	1.86	26.3	0	2
6	251.08	2	0	2.66	26.3	1	2
7	248.28	2	0	3.53	26.3	2	2
8	281.1	3	0	2.63	35.53	2	3
9	308.33	4	0	3.44	44.76	4	4
10	281.1	3	0	2.65	35.53	2	3
11	308.33	4	0	3.49	44.76	4	4
12	281.1	3	0	2.64	35.53	2	3
13	308.33	4	0	3.5	44.76	4	4
14	269.07	3	0	2.97	26.3	1	3
15	284.26	4	0	4.15	26.3	2	4
16	384.27	8	0	5.6	26.3	4	8
17	296.07	4	0	1.87	72.12	2	4
18	296.07	4	0	1.86	72.12	2	4
19	280.27	4	2	2.69	66.76	2	6
21	267.9	2	0	2.22	26.3	0	2
22	267.9	2	0	2.1	26.3	0	2
23	262.3	2	0	3.88	26.3	2	2
24	262.3	2	0	3.76	26.3	2	2
25	398.3	8	0	5.96	26.3	4	8
26	398.3	8	0	5.84	26.3	4	8
27	327.17	2	0	4.12	26.3	2	2
28	387.22	4	0	4.08	44.76	4	4
29	363.15	4	0	4.73	26.3	2	4
30	463.17	8	0	6.18	26.3	4	8
31	284.39	2	0	5.09	26.3	6	2
32	312.45	2	0	5.66	26.3	8	2
33	356.37	4	0	4.19	44.76	2	4
34	164.97	2	0	1.66	26.3	0	2
35	256.43	2	0	1.81	26.3	0	2
36	206.63	2	0	2.56	26.3	1	2
37	236.65	3	0	2.54	35.53	2	3
38	251.62	4	0	1.77	72.12	2	4
39	346.8	2	0	2.44	26.3	1	2
41	501.19	6	1	2.77	116.23	10	7

Conclusion

A library of bromine-, chlorine- and iodine-containing furanones was prepared using a variety of Pd-mediated coupling reactions. This library was subsequently screened for its effect on QS-regulated bioluminescence in *V. harveyi*. Several compounds were highly effective in inhibiting luminescence with up to 81% inhibition recorded for the most potent molecule. While highly brominated compounds were generally more active, chlorine- and iodine-containing derivatives were also associated with increased potential for QS inhibition. Finally, most of the library had a limited effect on bacterial growth, highlighting their potential as QS inhibitors.

Future Perspective

The discovery of antibiotics remains one of the crowning achievements of the 20th century. However, since their introduction, the problem of antimicrobial resistance has grown exponentially, with ever more cases of resistant infections being reported in the literature. Diseases caused by resistant bacteria now constitute the second most common cause of death globally [51]. Coupled to this, few new classes of antibiotics have been identified over the past 50 years with an ever smaller number of pharmaceutical companies willing to invest in this field. Some measures have been implemented to limit the spread of antimicrobial resistance (AMR), mostly notably the EU-mandated ban on the use of antibiotics as growth promoters in animal husbandry [52]. However, the continued growth of AMR suggests that such efforts may be “too little, too late”. The situation has been further exacerbated by the COVID-19 pandemic with the World Health Organisation (WHO) recently issuing warnings against the inappropriate use of antibiotics to treat COVID-19 infections. Evidence suggests that approximately 15% of severely ill COVID-19 patients develop bacterial co-infections and would benefit from antibiotics [53]. In reality, up to 75% of such patients are actually prescribed antibiotics. The WHO has also highlighted the long term implications of endemic COVID-19, with an urgent need for new diagnostic tools to differentiate bacterial and viral infections [54].

It is clear that a multipronged approach to tackling AMR is required. The use of small molecule inhibitors of QS (quorum quenching) has long been touted as one promising strategy with untapped potential. Interference with cell-cell communication offers a unique opportunity to regulate bacterial virulence and polymicrobial infections without exerting additional pressure to select for resistance. By disrupting bacterial resistance mechanisms, these compounds, used in conjunction with immunostimulants, could help the body to clear an infection without recourse to bactericidal agents. Additionally, these inhibitors should have limited impact on beneficial bacterial flora, thus promoting a healthier microbiome.

In spite of the many advantages outlined above, a number of questions remain unresolved. Firstly, it has yet to be demonstrated that QS inhibition is effective in a clinical setting. It is also unclear how well QS inhibitors would fare against a well-established infection. Lastly, the plethora of different QS

families and the varied responses of different strains to the same compounds makes it challenging to develop effective, broad spectrum inhibitors. Thus, while research to date is highly promising, there remains a long road ahead.

Acknowledgements

TL is grateful to the School of Pharmacy, University College Cork and Future University Egypt for financial support. CGMG acknowledges support from Science Foundation Ireland in the form of a center grant (APC Microbiome Ireland grant SFI/12/RC/2273_P2).

Financial and competing interests disclosure

The authors have no other relevant affiliations or financial involvement with any organization or entity with a financial interest in or financial conflict with the subject matter or materials discussed in the manuscript apart from those disclosed.

No writing assistance was utilized in the production of the manuscript.

Summary Points

-A library of bromine-, chlorine- and iodine-containing furanones was prepared and subjected to further modification *via* Pd-catalysed coupling reactions.

-Several compounds in this library were found to strongly inhibit quorum sensing-regulated bioluminescence in *V. harveyi*.

-Highly brominated furanone structures were associated with increased inhibitory activity, with tribromofuranone **39** proving the most active molecule.

-Dichlorofuranone **34** was biologically active confirming that the presence of bromine was not a prerequisite for activity.

-Screening of the library *in silico* did not identify any candidates which violated Lipinski's or Veber's rules.

CORRESPONDING AUTHOR

Timothy P. O'Sullivan (Tim.OSullivan@ucc.ie).

References

Papers of special note have been highlighted as: * of interest; ** of considerable interest

1. Austin B, Zhang X-H. *Vibrio harveyi* : a significant pathogen of marine vertebrates and invertebrates*. Lett. Appl. Microbiol.* 43(2), 119-124 (2006).
2. Lavilla-Pitogo CR, Leano EM, Paner MG. Mortalities of pond-cultured juvenile shrimp, *Penaeus monodon*, associated with dominance of luminescent vibrios in the rearing environment. *Aquacult.* 164(1-4), 337-349 (1998).
3. Austin B, Pride AC, Rhodie GA. Association of a bacteriophage with virulence in *Vibrio harveyi. J. Fish Dis.* 26(1), 55-58 (2003).
4. Diggles BK, Moss GA, Carson J, Anderson CD. Luminous vibriosis in rock lobster *Jasus verreauxi* (Decapoda: Palinuridae) phyllosoma larvae associated with infection by *Vibrio harveyi. Dis. Aquat. Organ.* 43(2), 127-137 (2000).
5. Pragyan Dash P, Avunje S, Ritesh S. Tandel RS, Sandeep KP, Akshaya Panigrahi A. Biocontrol of Luminous Vibriosis in Shrimp Aquaculture: A Review of Current Approaches and Future Perspectives*. Rev. Fish. Sci. Aquac* 25(3), 245-255 (2017).
6. Karunasagar I, Otta SK, Karunasagar I. Biofilm formation by *Vibrio harveyi* on surfaces*. Aquac.* 140(3), 241-245 (1996).
7. Olson ME, Ceri H, Morck DW, Buret AG, Read RR. Biofilm bacteria: formation and comparative susceptibility to antibiotics*. Can. J. Vet. Res.* 66(2), 86-92 (2002).
8. Bassler BL. How bacteria talk to each other: regulation of gene expression by quorum sensing*. Curr. Opin. Microbiol.* 2(6), 582-587 (1999).
9. Bassler BL, Wright M, Showalter RE, Silverman MR. Intercellular signalling in *Vibrio harveyi*: sequence and function of genes regulating expression of luminescence*. Mol. Microbiol.* 9(4), 773-786 (1993).
10. Rutherford ST, Bassler BL. Bacterial Quorum Sensing: Its Role in Virulence and Possibilities for Its Control*. Cold Spring Harbor Perspectives in Medicine* 2(11), a012427 (2012).
11. Papenfort K, Bassler BL. Quorum sensing signal-response systems in Gram-negative bacteria*. Nat. Rev. Microbiol.* 14(9), 576-588 (2016).
12. Galloway WRJD, Hodgkinson JT, Bowden SD, Welch M, Spring DR. Quorum Sensing in Gram-Negative Bacteria: Small-Molecule Modulation of AHL and AI-2 Quorum Sensing Pathways*. Chem. Rev.* 111(1), 28-67 (2011).

****Overview of quorum sensing in Gram-negative bacteria**

13. Defoirdt T. Quorum-sensing systems as targets for antivirulence therapy*. Trends Microbiol.* 26(4), 313-328 (2017).

14. Plener L, Lorenz N, Reiger M *et al*. The phosphorylation flow of the *Vibrio harveyi* quorum-sensing cascade determines levels of phenotypic heterogeneity in the population*. J. Bacteriol.* 197(10), 1747-1756 (2015).
15. Anetzberger C, Reiger M, Fekete A *et al*. Autoinducers act as biological timers in *Vibrio harveyi. PLOS ONE* 7(10), e48310 (2012).
16. Waters CM, Bassler BL. Quorum sensing: cell-to-cell communication in bacteria*. Annu. Rev. Cell. Dev. Biol.* 21 319-346 (2005).
17. Fleitas Martínez O, Rigueiras PO, Pires ÁDS *et al*. Interference With Quorum-Sensing Signal Biosynthesis as a Promising Therapeutic Strategy Against Multidrug-Resistant Pathogens*. Frontiers in Cellular and Infection Microbiology* 8 444 (2019).
18. Kazlauskas R, Murphy PT, Quinn RJ, Wells RJ. A new class of halogenated lactones from the red alga *delisea fimbriata* (bonnemaisoniaceae)*. Tetrahedron Letters* 18(1), 37-40 (1977).
19. De Nys R, Wright AD, König GM, Sticher O. New halogenated furanones from the marine alga *delisea pulchra* (*cf. fimbriata*)*. Tetrahedron* 49(48), 11213-11220 (1993).
20. Dworjanyn SA, Nys RD, Steinberg PD. Chemically mediated antifouling in the red alga *Delisea pulchra. Mar. Ecol. Prog. Ser.* 318 153-163 (2006).
21. Ranall MV, Butler MS, Blaskovich MA, Cooper MA. Resolving biofilm infections: current therapy and drug discovery strategies*. Curr. Drug Targets* 13(11), 1375-1385 (2012).
22. Givskov M, De Nys R, Manefield M *et al*. Eukaryotic interference with homoserine lactone-mediated prokaryotic signalling*. J. Bacteriol.* 178(22), 6618-6622 (1996).
23. De Nys R, Steinberg P, Willemsen P, Dworjanyn S, Gabelish C, King R. Broad spectrum effects of secondary metabolites from the red alga *delisea pulchra* in antifouling assays*. Biofouling* 8(4), 259–271 (1995).
24. Zang T, Lee BWK, Cannon LM *et al*. A naturally occurring brominated furanone covalently modifies and inactivates LuxS*. Bioorg. Med. Chem. Lett* 19(21), 6200-6204 (2009).
25. Zhu J, Patel R, Pei D. Catalytic Mechanism of *S*-Ribosylhomocysteinase (LuxS): Stereochemical Course and Kinetic Isotope Effect of Proton Transfer Reactions*. Biochemistry* 43(31), 10166-10172 (2004).

26. Defoirdt T, Benneche T, Brackman G, Coenye T, Sorgeloos P, Scheie AA. A quorum sensing-disrupting brominated thiophenone with a promising therapeutic potential to treat luminescent vibriosis*. PloS one* 7(7), e41788 (2012).
27. Lyons T, Gahan CGM, O'Sullivan TP. Structure–activity relationships of furanones, dihydropyrrolones and thiophenones as potential quorum sensing inhibitors*. Future Med. Chem.* 12(21), 1925-1943 (2020).

***Survey of structure activity relationships of furanones and related compounds**

28. Proctor CR, Mccarron PA, Ternan NG. Furanone quorum-sensing inhibitors with potential as novel therapeutics against *Pseudomonas aeruginosa. J. Med. Microbiol.* 69(2), 195-206 (2020).
29. Markus V, Golberg K, Teralı K *et al*. Assessing the Molecular Targets and Mode of Action of Furanone C-30 on *Pseudomonas aeruginosa* Quorum Sensing*. Molecules* 26(6), 1620 (2021).
30. Defoirdt T, Crab R, Wood TK, Sorgeloos P, Verstraete W, Bossier P. Quorum Sensing-Disrupting Brominated Furanones Protect the Gnotobiotic Brine Shrimp *Artemia franciscana* from Pathogenic *Vibrio harveyi*, *Vibrio campbellii*, and *Vibrio parahaemolyticus* Isolates*. Appl. Environ. Microbiol.* 72(9), 6419-6423 (2006).
31. Gómez A-C, Lyons T, Mamat U *et al*. Synthesis and evaluation of novel furanones as biofilm inhibitors in opportunistic human pathogens*. Eur. J. Med. Chem.* 242 114678 (2022).
32. Riedel CR, Monk IR, Casey PG *et al*. Improved Luciferase Tagging System for *Listeria monocytogenes* Allows Real-Time Monitoring In Vivo and In Vitro*. Appl. Environ. Microbiol.* 73(9), 3091-3094 (2007).
33. Bassler BL, Wright M, Silverman MR. Multiple signalling systems controlling expression of luminescence in *Vibrio harveyi*: sequence and function of genes encoding a second sensory pathway. *Mol. Microbiol.* 13(2), 273-286 (1994).
34. Lyons T, Gahan CGM, O'Sullivan TP. Synthesis and reactivity of dihalofuranones*. Lett. Org. Chem.* 19(8), 662-667 (2022).
35. Janssens JCA, Steenackers H, Robijns S *et al*. Brominated Furanones Inhibit Biofilm Formation by *Salmonella enterica Serovar Typhimurium. Appl. Environ. Microbiol.* 74(21), 6639-6648 (2008).
36. Steenackers HP, Levin J, Janssens JC *et al*. Structure-activity relationship of brominated 3-alkyl-5-methylene-2(5*H*)-furanones and alkylmaleic anhydrides as

inhibitors of *Salmonella* biofilm formation and quorum sensing regulated bioluminescence in *Vibrio harveyi. Bioorg. Med. Chem.* 18(14), 5224-5233 (2010).

37. Han Y, Hou S, Simon KA, Ren D, Luk Y-Y. Identifying the important structural elements of brominated furanones for inhibiting biofilm formation by *Escherichia coli. Bioorg. Med. Chem. Lett.* 18(3), 1006-1010 (2008).
38. Biswas NN, Iskander GM, Mielczarek M, Yu TT, Black DS, Kumar N. Alkyne-Substituted Fimbrolide Analogues as Novel Bacterial Quorum-Sensing Inhibitors*. Aust. J. Chem.* 71(9), 708-715 (2018).
39. Goh WK, Gardner CR, Chandra Sekhar KV *et al*. Synthesis, quorum sensing inhibition and docking studies of 1,5-dihydropyrrol-2-ones*. Bioorg. Med. Chem.* 23(23), 7366-7377 (2015).
40. Goh WK, Iskander G, Black DS, Kumar N. An efficient lactamization of fimbrolides to novel 1,5-dihydropyrrol-2-ones*. Tetrahedron Lett.* 48(13), 2287-2290 (2007).
41. Zhao G, Wan W, Mansouri S *et al*. Chemical synthesis of *S*-ribosyl-L-homocysteine and activity assay as a LuxS substrate*. Bioorg. Med. Chem. Lett.* 13(22), 3897-3900 (2003).
42. Mina G, Chbib C. Recent progresses on synthesized LuxS inhibitors: A mini-review*. Bioorg. Med. Chem. Lett.* 27(1), 36-42 (2019).
43. Alfaro JF, Zhang T, Wynn DP, Karschner EL, Zhou ZS. Synthesis of LuxS inhibitors targeting bacterial cell-cell communication*. Org. Lett.* 6(18), 3043-3046 (2004).
44. Li X, Li H, Yang W, Zhuang J, Li H, Wang W. A mild and selective protecting and reversed modification of thiols*. Tetrahedron Lett.* 57(24), 2660-2663 (2016).
45. Meot-Duros L, Cérantola S, Talarmin H, Le Meur C, Le Floch G, Magné C. New antibacterial and cytotoxic activities of falcarindiol isolated in *Crithmum maritimum* L. leaf extract*. Food Chem. Toxicol.* 48(2), 553-557 (2010).
46. Mcphail KL, Correa J, Linington RG *et al*. Antimalarial Linear Lipopeptides from a Panamanian Strain of the Marine Cyanobacterium *Lyngbya majuscula. J. Nat. Prod.* 70(6), 984-988 (2007).
47. Lee MD, Ellestad GA, Donald B. Borders DB. Calicheamicins: discovery, structure, chemistry, and interaction with DNA*. Acc. Chem. Res.* 24(8), 235-243 (1991).
48. Daina A, Michielin O, Zoete V. SwissADME: a free web tool to evaluate pharmacokinetics, drug-likeness and medicinal chemistry friendliness of small molecules*. Sci. Rep.* 7 42717 (2017).

49. Lipinski CA, Lombardo F, Dominy BW, Feeney PJ. Experimental and Computational Approaches to Estimate Solubility and Permeability in Drug Discovery and Development Settings. *Adv. Drug Del. Rev.* 46(1), 3-26 (2001).
50. Veber DF, Johnson SR, Cheng H-Y, Smith BR, Ward KW, Kopple KD. Molecular Properties That Influence the Oral Bioavailability of Drug Candidates. *J. Med. Chem.* 45(12), 2615-2623 (2002).
51. World Health Organisation. Antimicrobial Resistance: Global Report on Surveillance. *WHO Reports* (2014).
52. Cully M. Public health: The politics of antibiotics. *Nature* 509 S16–S17 (2014).
53. Di Guardo G. COVID-19: Measles and Antibiotic Resistance Are a Matter of Concern. *Pathogens* 10(4), 449 (2021).
54. World Health Organisation. Preventing the COVID-19 pandemic from causing an antibiotic resistance catastrophe. *WHO Reports* (2020).